The characterization of the severity of rotor delevitation events: A parametric study

Jan J. Janse van Rensburg*
School of Mechanical and Nuclear Engineering, North-West University, Potchefstroom, South-Africa

George van Schoor
Unit for Energy Systems, North-West University, Potchefstroom, South-Africa

Pieter A. van Vuuren
School of Electrical, Electronic and Computer Engineering, North-West University
Potchefstroom, South-Africa

Abstract

Active magnetic bearing (AMB) failure and the ensuing rotor behavior is a very important aspect of AMB safety. A model for this rotor behavior was developed and was used to characterize the severity of rotor delevitation events. The characterization was done by means of severity indicators derived from the rotor behavior within the backup bearings.

The indicator is a quantitative value that can be used to compare different delevitation events. The indicator presented in this paper is the non-dimensionalised velocity of the geometric center of the rotor (*Vval*).

This indicator only requires the rotational speed and position data of the rotor to determine the *Vval* quantity. This ensures that this value can be determined for most current operational systems and on historical data logged from previous rotor delevitation events.

In order to validate *Vval*, a comparison was done between simulated and experimental rotor drops and their associated *Vval* values. The model used to produce the simulation results is BBSim. Experimental results were obtained on a 4-axis suspended rotor, modified to use rolling element backup bearings.

1 Introduction

Backup bearing modeling is necessary in order to develop inherently safe AMB systems. This is the reasoning behind the development of BBSim [1]. BBSim accurately models the behavior of a rotor during levitation and during a rotor delevitation event. The BBSim model includes the following capabilities: flexible rotor modeling, contact dynamics, cross coupling of any number of backup bearings, inner race speed-up, rotor braking due to aerodynamic losses, rotor braking due to contact dynamics, active rotor braking, rotor non-circularity at the sensing and contact surfaces, a fully functioning AMB model, multi-plane rotor unbalance and stator dynamics. The developed rotor/AMB/Backup bearing system consists of four main sub-models: a rotor-model, AMB-models, backup bearing/stator-models in the translational direction and rotational backup bearing-models. The rotor, AMB, rotational model and translational backup bearing sub-models are shown in Figure 1.

The basic operation of the simulation model is that the translational backup bearing (BB) models receive the current position of the rotor from the rotor model. The BB model also receives the friction force from the friction model. The BB model also sends the reaction force to the rotor model. The friction model receives the normal forces acting on the rotor and uses them to determine the friction forces. It also receives the current bearing speed from the rotational BB model and sends the current friction factor to the rotational model. The rotational BB model receives the perpendicular forces from the friction model and determines the speed-up torque of the bearing and the slow-down torque of the rotor. It also receives the current friction factor from the friction model. The AMB model receives the current position of the rotor at the sensor locations and sends the forces acting on the rotor at the AMB locations. The rotor model receives the forces acting on the rotor (from AMBs and BBs) and sends the current position of the rotor (to the AMBs and BBs). It receives the current rotational speed from the rotational BB model. Although the model used to create the data used in this paper is more complex this paper does not focus on the bearing model. A detailed explanation of the model can be found in [1].

A consequence of the development of an accurate model was the need to quantify the dynamics of the rotor drop severity. To address this need a severity indicator was developed, similar to the one presented in [2]. This

*Email: Jan.JansevanRensburg@nwu.ac.za, Tel: +27823352295

indicator is the distance travelled by the geometric center of the rotor during a rotor drop divided with the airgap radius (*Vval*). The quantification of the severity enabled objective comparisons between rotor delevitation events. The objective comparison of delevitation events enabled parametric studies to be done. Some of these parametric studies are presented within this paper.

The first section of this paper discusses the rationale behind using the non-dimensionalised velocity of the geometric center of the rotor to quantify the rotor delevitation event severity.

In order to verify the quantification method, experimental and simulated values are compared. These results include the *Vval* values and the rotor orbit plots. Following the verification of the quantification method some parametric results are presented and discussed. The parametric studies include: stiffness, damping, rotational speed, friction, inertia of the inner race and balls of the bearing and the magnitude of the unbalance present in the system. Conclusions are made based on the presented parametric studies.

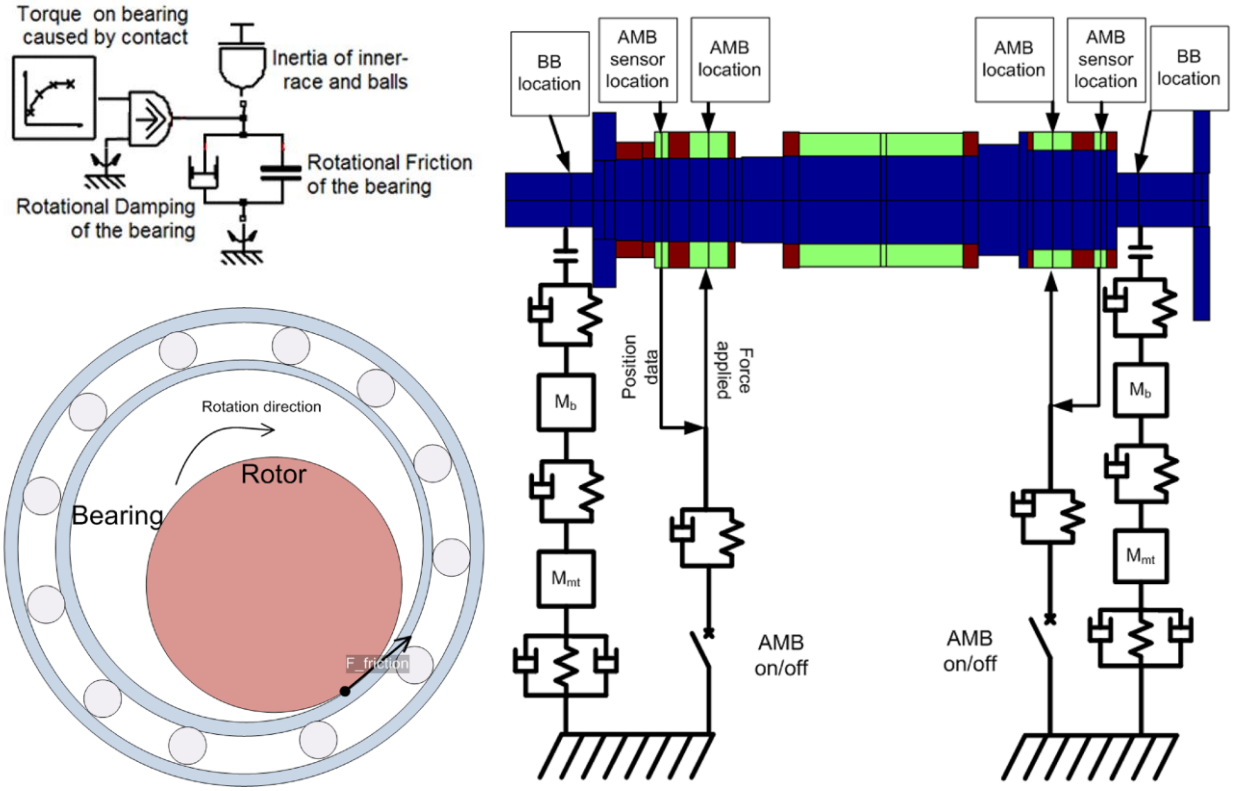

Figure 1: Translational and rotational model of backup bearings, AMBs and rotor

2 Rotor drop event severity quantification

The method to quantify rotor delevitation events is presented in this section. The rationale is to measure the amount of energy that is transformed into transverse motion. The energy is an indication of the impact that a certain rotor drop has on the degradation of the bearing-quality. An indication of the amount of energy that is transformed into transverse motion is the distance that the geometric center of the rotor travels within the backup bearing clearance.

This distance is then non-dimensionalised by dividing with the airgap radius in order to provide a number that represents the number of times that the rotor travelled the entire distance of the airgap as shown in Equation (1), with n the window size (number of samples), i the index number, r_{airgap} the radius of the backup bearing clearance, x the position of the rotor center in the x-direction, y the position of the rotor center in the y-direction, k the index number for *Dval* and n_{total} the total number of samples in the rotor delevitation event data.

This non-dimensionalised distance is then divided by the time over which it was calculated to produce an average non-dimensionalised speed with the unit per second. If the chosen window size is the same as the total

number of samples in the rotor delevitation event's data, there is only one *Dval* value. When the window size and total number of samples are the same Equation (2) is used to determine the *Vvala* value, with f_s the sampling frequency and n the window size (in this case 60 000 samples).

Should the window size be chosen smaller than the total number of samples in the data set, there is more than one *Dval* value. Of these *Dval* values only the largest value is used to determine the *Vval* value as shown in Equation (3).

Throughout this document *Vvala* is determined with a window size of 60 000 samples and a sampling frequency of 10 000 Hz. Similarly *Vval* is determined with a window size of 1 000 samples and a sampling frequency of 10 000 Hz.

$$Dval_k = \frac{\sum_{i=((k\cdot n)-n)+1}^{k\cdot n} \sqrt{\left(x_i - x_{i-1}\right)^2 + \left(y_i - y_{i-1}\right)^2}}{r_{airgap}} \text{ with } k = \left[1, \ldots, \frac{n_{total}}{n}\right] \tag{1}$$

$$Vvala = Dval_1 \cdot \left(\frac{f_s}{n}\right) = Dval_1 \cdot \left(\frac{f_s}{60000}\right) \tag{2}$$

$$Vval = \max\left(Dval_1 \cdot \left(\frac{f_s}{1000}\right), \ldots, Dval_k \cdot \left(\frac{f_s}{1000}\right)\right) \tag{3}$$

These values are then used to determine the severity of a rotor drop either as it is taking place, or on previously captured data, or on simulation results. In essence Equation (1) is a derivative operation, thus it exaggerates the noise present on the position data and for this reason an average value is used (with differing window sizes). Filters could also be employed but since the idea of this method is to be able to do real time calculations, the computational effort should be as little as possible. The real-time calculation of this value will enable safe rotor-drop tests where the rotor can be re-levitated once a safe-threshold value has been reached or exceeded.

3 Simulated and experimental results comparison

In this section the *Vval* and *Vvala* values for experimental and simulated results are compared in order to validate the simulation model. Also presented are visual comparisons between experimental and simulated rotor orbit plots. These orbit plots show similar rotor behavior and serves as further validation of the simulation model.

The *Vval* and *Vvala* values are used as a quantitative value to compare the results of the simulations with the experimental results. As with most theoretical results there are discrepancies between the experimental and simulated results. These discrepancies are attributed to the highly non-linear nature of bearing problems, the uncertainty of certain simulation parameters and the presence of noise on the experimental results.

A secondary method to compare results, albeit qualitative, is to visually compare rotor orbit plots from experimental and simulated data with each other. This method is subjective but still valuable in identifying similar overall rotor behavior.

The experimental results were obtained on a 4-axis supported rotor as described in [3] modified to operate on two rolling element backup bearings. Bearing 1 is located on the left side of the system and bearing 2 on the right side of the system.

3.1 *Vval* value comparison

In Figure 2 experimental data from 49 separate rotor drops is used to calculate the *Vvala* value of each delevitation event, these values are then compared with *Vvala* values calculated from simulation data. It is important to note that in Figure 2 the window size used to calculate *Vvala* is 60 000 samples. This means that it is the average *Vval* value for a rotor drop that lasted 6 seconds.

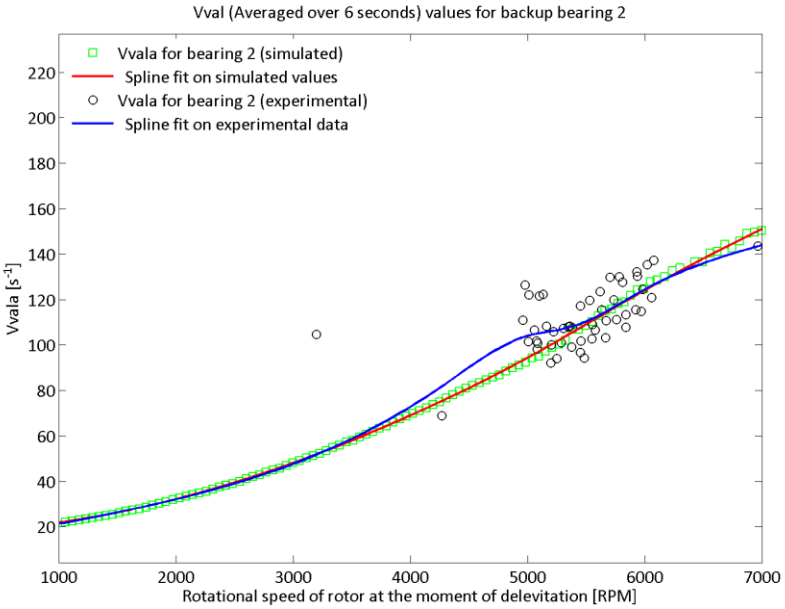

Figure 2: Comparison of *Vval* values between experimental and simulated results for bearing 2 (n = 60 000, f_s = 10 000 [Hz])

The same experimental and simulated data were used in Figure 3 with a reduced window size of 1 000 samples. In effect this means that each rotor drop produced 60 different *Vval* values and that of these 60 *Vval* values only the maximum value is plotted in Figure 3. The rationale behind this is to emphasize short periods of high bearing loads. It would be good practice to use both these window sizes when deciding whether a rotor drop should be considered safe or not.

From Figure 2 and Figure 3 it can be seen that the agreement between the simulated results and the experimental results is satisfactory. Thus the model can be used to simulate AMB failure and the ensuing rotor bearing interaction.

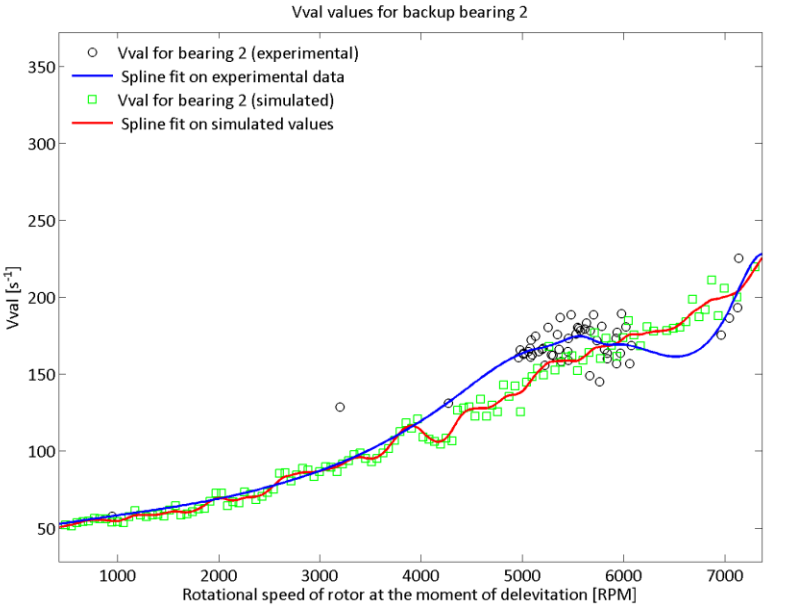

Figure 3: Comparison of *Vval* values between experimental and simulated results for bearing 2 (n = 1 000, f_s = 10 000 [Hz])

3.2 Visual results comparison

To further compare simulated and experimental results a visual comparison between rotor orbit plots is given in this section. Some selected results are presented showing different rotor behaviors during different initial conditions and comparing them with similar simulated results. It is important to note that not all parameters of the simulation and the experimental results are the same. The stiffness and damping of the bearing and bearing housing could not be measured accurately, thus the experimental results and simulated results does not look exactly the same, but the behavior of the rotor orbits is important to note. The similar behavior mentioned is: minimal rocking motion, rocking motion, rocking motion with small bounces, rocking motion leaning towards forward whirling, short duration forward whirling and a longer duration forward whirling.

Figure 4 shows the rotor orbit plot comparison for a rotor drop where the rotational speed of the rotor at the moment of delevitation was 1173 [RPM]. Comparing the simulated and experimental results for bearing 1 (the two plots on the left side of the figure) shows that the simulated and experimental results has similar behavior, in particular note the first bounce of the rotor. It is also important to note the presence of noise in the experimental results. Comparing bearing 2 also reveals similar behavior, after initial contact the rotor bounces to the right of the clearance circle, and then settles to a rocking motion with relatively small amplitude.

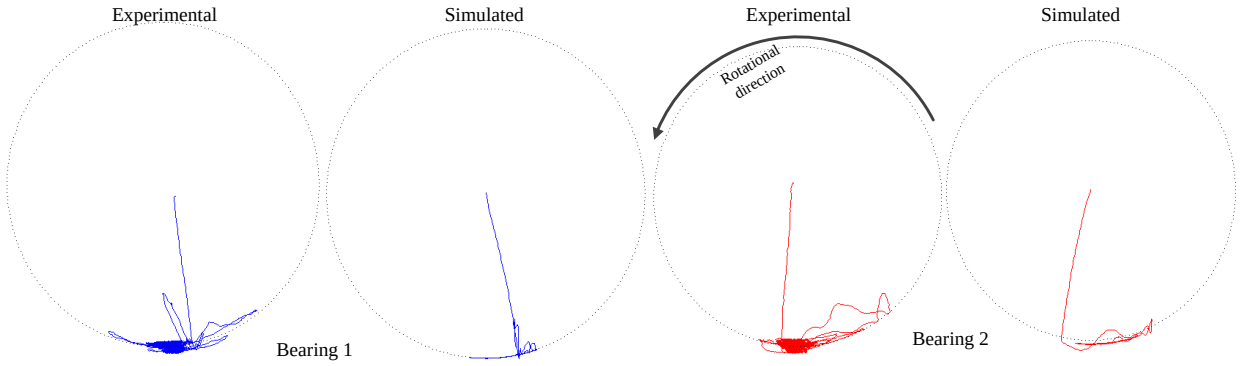

Figure 4: Orbit plot comparison for a rotor drop speed of 1173 [RPM] (minimal rocking motion)

In Figure 5 similar results is shown with the exception that the rotor drop speed was higher. Once again note the presence of noise in the experimental results. The comparison between simulated and experimental results for bearing 1 show once again very similar results for the experimental and simulated results, with the exception of the amplitude of the rocking motion. The difference in amplitude of the rocking motion is attributed to the fact that the bearing and bearing holder stiffness and damping values in the simulation differ from the real values, and secondly that the damping value present in the simulation of bearing 2 is too high. The excessively high damping value used for bearing 2 in the simulation not only effects the behavior of bearing 1 but also the explains the lower amplitude of the first bounce and the lower amplitude of the rocking motion present in bearing 2. The bearing characteristics and rotor behavior for bearing 1 influences the rotor behavior at bearing 2, and vice versa, due to cross-coupling.

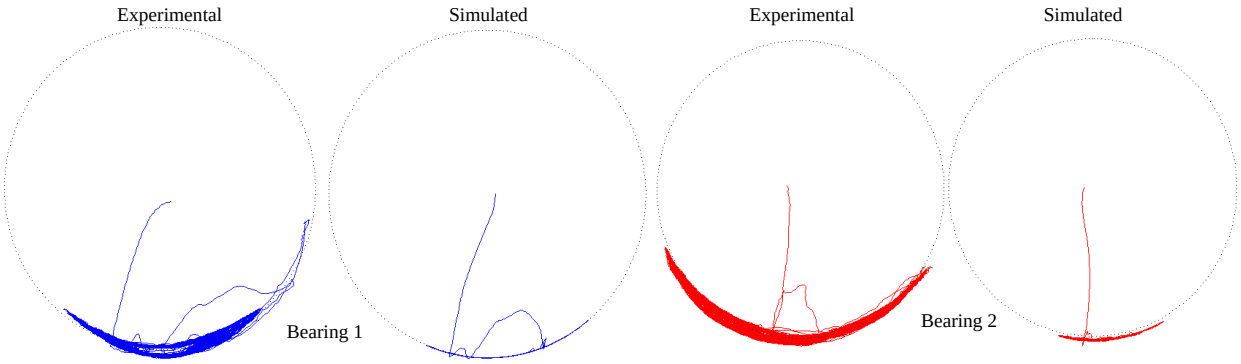

Figure 5: Orbit plot comparison for a rotor drop speed of 2201 [RPM] (rocking motion)

Figure 6 shows the rotor orbit plots for a rotational speed of 4589 [RPM]. In comparison the experimental and simulated results of bearing 1 seems similar, with the exception of the small bounces on the left side of the orbit plot of the simulated results, this is again attributed to the fact that the stiffness and damping characteristics of the of the simulated model do not exactly match those of the experimental setup. When examining the results of bearing 2 it is once again clear that the amplitude of the experimental result's rocking motion is larger than the simulated results. This is due to an excessively large damping present in the simulation model. The simulation and experimental results shows a rocking motion for both bearing 1 and bearing 2

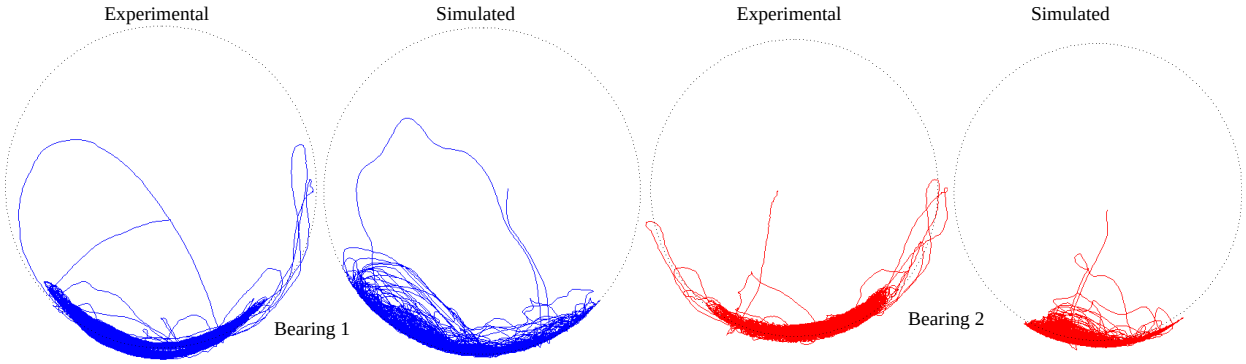

Figure 6: Orbit plot comparison for a rotor drop speed of 4589 [RPM]
(rocking motion with small bounces)

The results of a rotor drop with a drop speed of 5097 [RPM] is shown in Figure 7. Comparing the rotor behavior at bearing 1 clearly shows that both the simulation and the experimental results predict a tendency to go into a forward whirling motion, but both only experience a period of bouncing, and then settle to a rocking motion. An excessively large damping is again present in the simulation model of bearing 2.

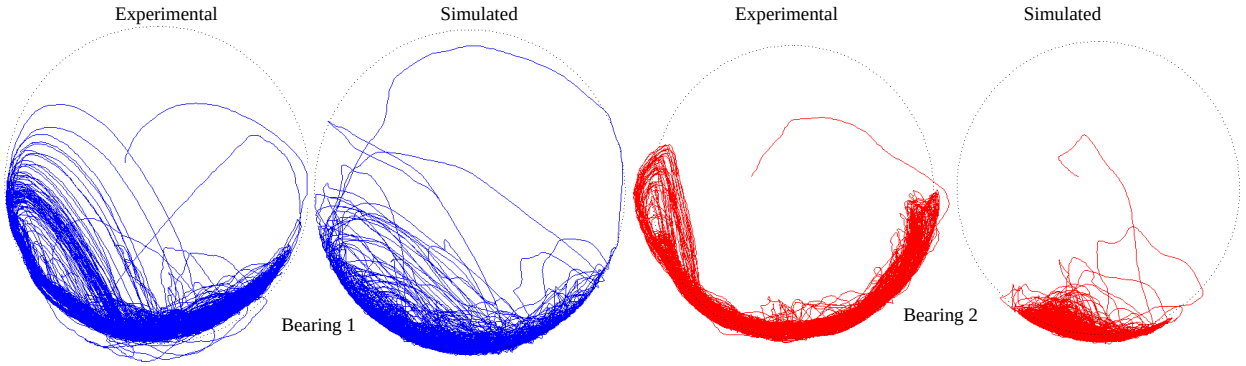

Figure 7: Orbit plot comparison for a rotor drop speed of 5097 [RPM]
(rocking motion leaning towards forward whirling)

In Figure 8 orbit plots of the results for a rotor dropped at 5547 [RPM] are presented. The results of bearing 1 show that both simulated and experimental rotors experience a period of forward whirling settling to a bouncing and then a rocking motion. Bearing 2 shows the influence of the impacts at bearing 1 on the orbits of bearing 2 (higher amplitude bouncing in the center of the bearing clearance, present in bearing 2).

Figure 9 is similar to Figure 8 with the exception that the period of forward whirling in bearing 1 lasts longer and is more pronounced than that for the similar behavior for the lower speed drop presented in Figure 8. When examining the results for bearing 2 it is clear that the impacts at bearing 1 has an influence on the rotor behavior at bearing 2 similar to that seen in Figure 8.

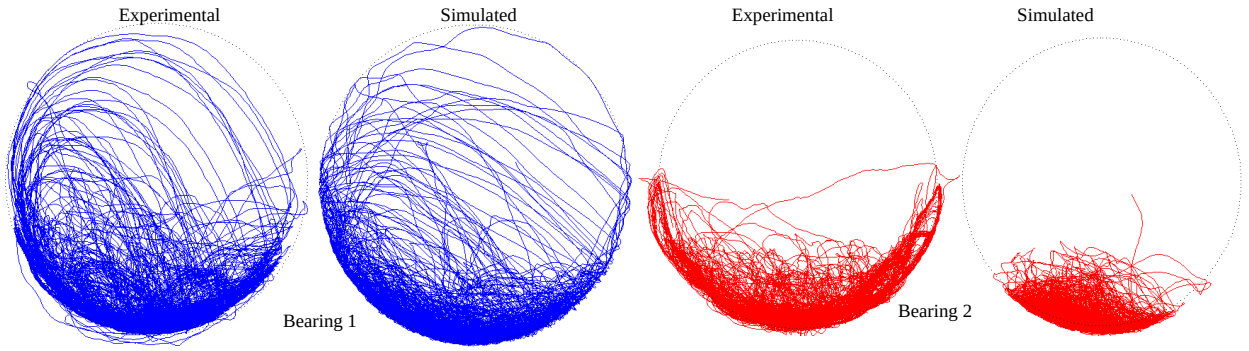

Figure 8: Orbit plot comparison for a rotor drop speed of 5547 [RPM]
(short duration forward whirling)

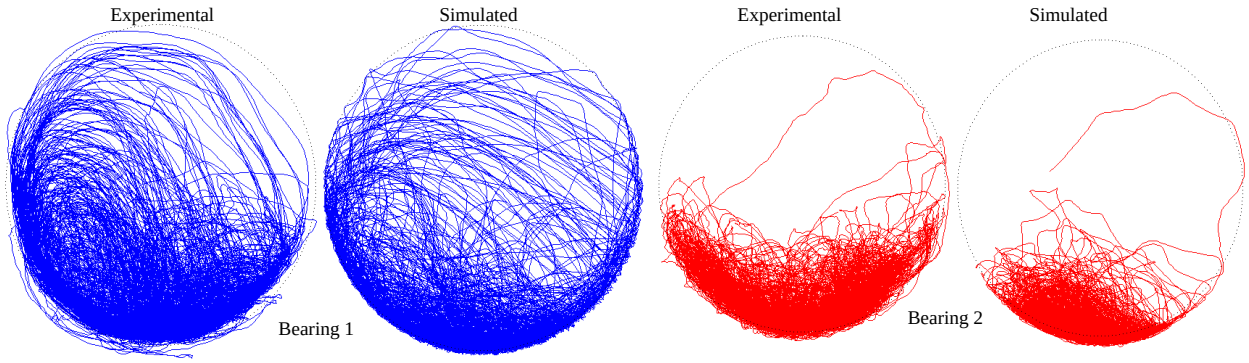

Figure 9: Orbit plot comparison for a rotor drop speed of 5883 [RPM]
(longer duration forward whirling)

Figures 4-9 show similar behavior of the rotor for various movement regimes, these results in conjunction with the results presented in Figure 2 and 3 is sufficient to assume that the simulation model is validated. The validation of the simulation model enables a parametric study on the system in question [3]. Some of the results of this parametric study are presented in the next section.

4 Parametric studies using BBSim

An important advantage of having a validated model is the ability to predict the behavior of a rotor during a rotor drop, and using the model to examine how the different parameters influence the rotor behavior. The influencing parameters examined in this section include bearing stiffness, bearing damping, delevitation angle, friction, magnitude of unbalance and the inertia of the inner race and balls of the bearing.

4.1 Bearing stiffness and damping

The parametric studies were done for 3 different initial speeds and varying the bearing stiffness and damping characteristics. A total of 1200 simulations each simulation representing 7 seconds of real world time was done. In the simulations the AMBs is switched off after 1 second. This is done in order to let the transients of the AMBs settle. Thus after the AMBs were switched off there was a rotor drop event that was simulated for 6 seconds.

These 6 second simulation results were post-processed in order to produce the *Vvala* and *Vval* values for each rotor drop event. The *Vvala* and *Vval* values were then used to produce 6 different surface plots, one set of 3 (one for each speed) for the *Vvala* values and one set of 3 for the *Vval* values. The 3 axes of the plot are the stiffness and the damping and the third axis is either the *Vvala* or the *Vval* value. These plots give some insight into how these parameters influence the rotor's behavior and using these a few design principles can be obtained.

Figure 10 shows the sensitivity of *Vval* to the bearing stiffness. It is important to note that the six surface plots shown in Figure 10 only show the maximum value of *Vval* (with a window size of 1000 samples at 10 000 Hz) at a

certain damping and stiffness. These graphs show whether there are short periods of destructive behavior. The higher the *Vval* value the more destructive the behavior. The graph clearly shows that the behavior is more sensitive to the damping of the system compared to the stiffness of the system. While a higher damping is preferable, the stiffness of the system influences the behavior of the rotor due to rotordynamic harmonics and is dependent on the rotor in question. Thus a similar range statement cannot be made of the stiffness of the system, since the ideal stiffness will vary depending on the rotordynamic characteristics of the rotor in question. Generally it can be stated that excessively high and excessively low stiffnesses should be avoided.

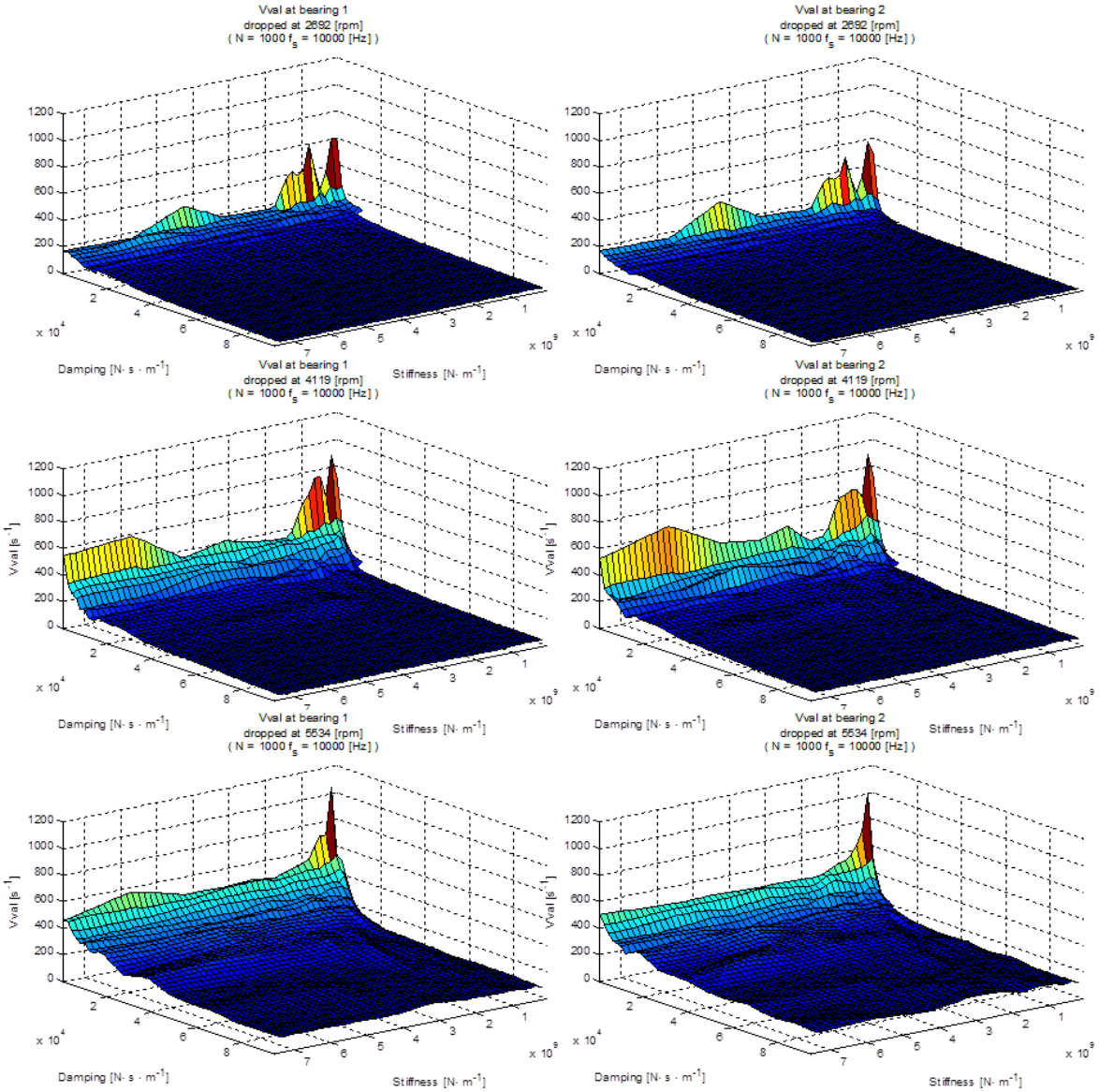

Figure 10: Rotor drop severity sensitivity to bearing stiffness and damping at three different rotational speeds (6 second rotor drop, maximum value of *Vval* with a window size of 1000 samples at 10 000 Hz)

Figure 11 shows the same 6 surface plots as in Figure 10 with the exception that the *Vval* was determined with a window size of 60 000 samples again at a sampling frequency of 10 000 Hz. From these plots it is clear that the increased window size has an averaging effect, this means that the results obtained with a larger window size shows the average severity of a rotor drop event, averaging out short periods of violent rotor behavior. From these results it is once again clear that the rotor behavior is more sensitive to the system damping when compared to the stiffness. The rotordynamic harmonics due to the variation of the stiffness of the system are also less visible in these results

since the rotor speeds down through the critical frequency and the result of the behavior of the rotor during this period is averaged out by the rest of the rotor behavior not near a critical frequency.

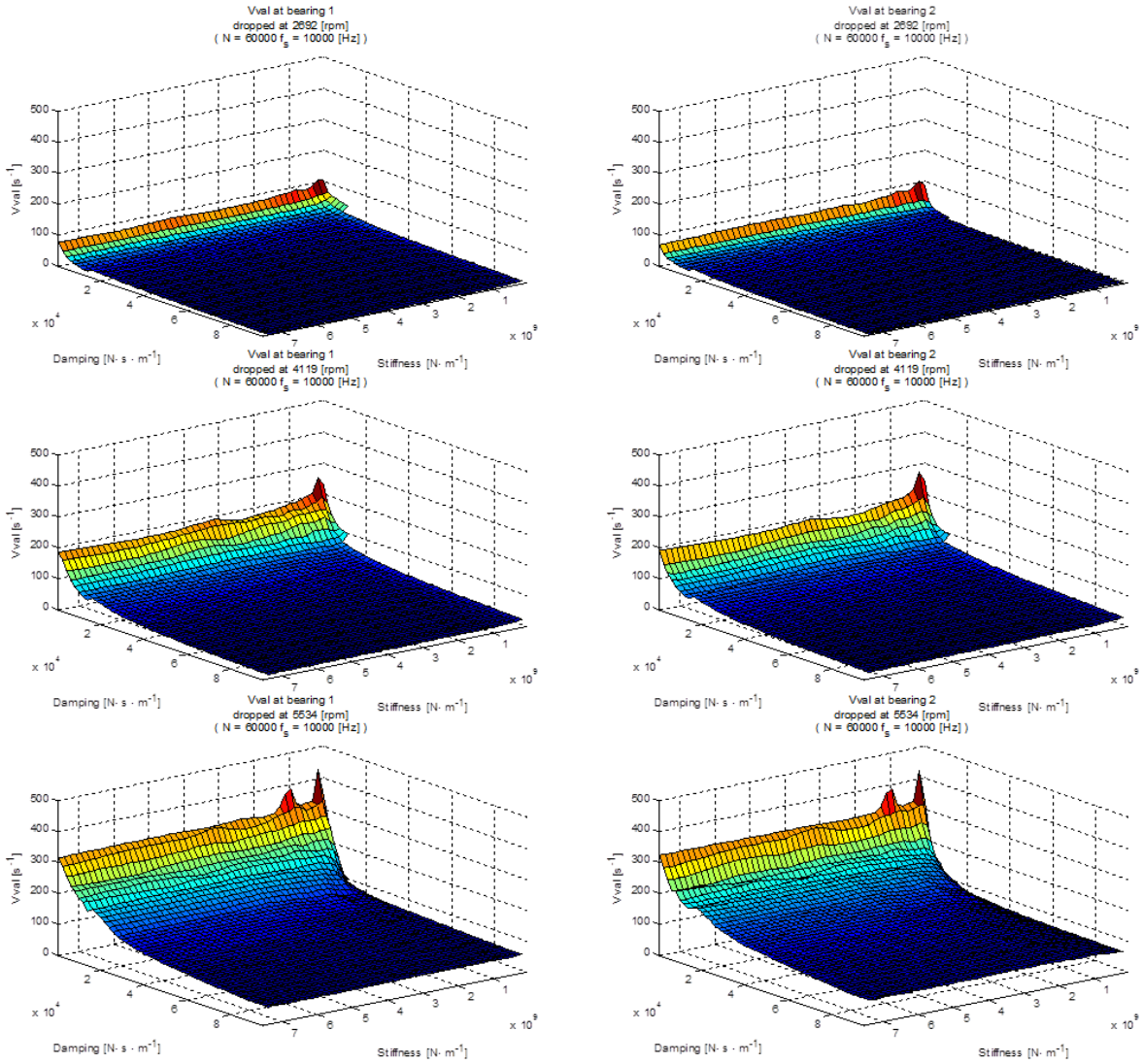

Figure 11: Rotor drop severity sensitivity to bearing stiffness and damping at three different rotational speeds (6 second rotor drop, *Vval* with a window size of 60 000 samples at 10 000 Hz)

The results from Figure 10 and Figure 11 are both important when determining the optimal bearing system stiffness and damping. Where the smaller window size (Figure 10) is important in choosing appropriate bearing system stiffness and the larger window size (Figure 11) is important in determining an appropriate bearing system damping.

4.2 Delevitation angle

The delevitation angle is the angle the center of mass of the rotor is at relative to the geometric center of the backup bearing clearance (at the moment of delevitation) as shown in Figure 12. The reasoning behind including this parametric study is to determine the impact that the location of the rotor, relative to the geometric center of the backup bearing clearance, has on the behavior of the rotor.

Shown in Figure 13 are four surface plots showing the sensitivity for the angle of delevitation and rotational speed of the rotor. The top two figures are once again for the smaller window size of 1000 samples, while the

bottom two figures are for a window size of 60 000 samples. The results for bearing 1 are shown on the left while the results for bearing 2 are shown on the right.

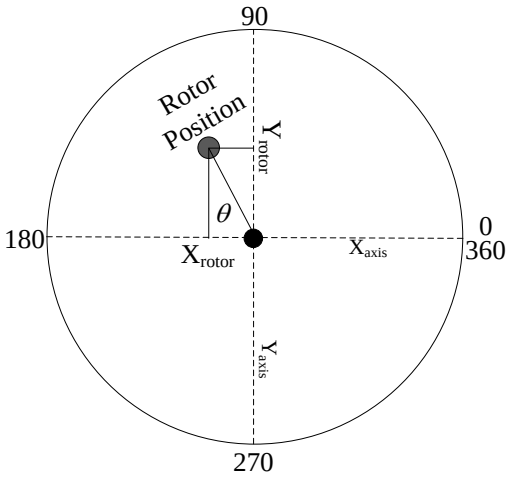

Figure 12: Delevitation angle

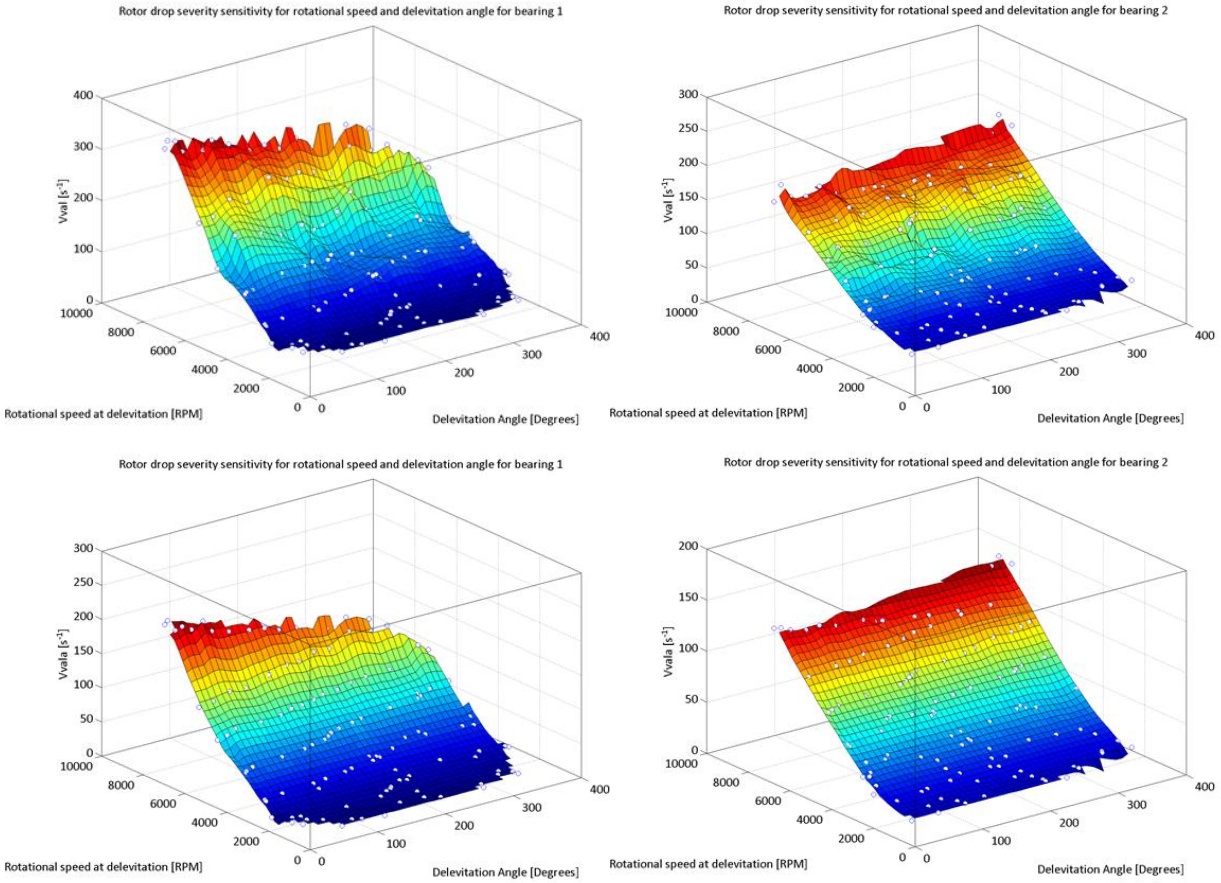

Figure 13: Delevitation angle sensitivity

From the first two surface graphs it appears that the rotor behavior is independent of the delevitation angle. It is however clear that the rotational speed has a large influence on the behavior of the rotor, where higher speeds produces more destructive behavior, as is expected. When examining the bottom two surface plots, a small but

noticeable influence on the behavior is noted. If the rotor is delevitated near 0 or 360 degrees, as shown in Figure 12 larger *Vval* and *Vvala* values are produced.

4.3 Friction, inertia and unbalance

Shown in Figure 14 (A) is the sensitivity of the rotor behavior to the friction factor between the rotor contact surface and the inner race of the rolling element bearing. Figure 14 (B) shows the sensitivity to the inertia of the inner race and rolling elements of the rolling element bearing. In Figure 14 (C) the sensitivity of the rotor behavior to the magnitude of the unbalance present on the rotor is shown.

The graphs were created by keeping all the variables constant except for the one in question and simulating a rotor delevitation event where the active magnetic bearings were turned off after one second and then lasted for 6 seconds. The resulting data was then post-processed to produce *Vval* (window size 1000) and *Vvala* (window size 60 000) values for each rotor drop for both bearings in the system.

Investigating the first graph (A) the results show that the rotor is relatively insensitive towards changes in the friction between the rotor inner race and the backup bearing. It is however important to note that this is only valid for rolling element bearings since the increased friction factor between the contacting surfaces causes the rotor and bearings to reach the same rotational speed in a shorter time period. This also slows down the rotor faster until the same rotational speed is reached by the rotor and the inner race. In effect braking the rotor initially thus producing a slightly less violent reaction when observing the *Vvala* value. The *Vvala* value for both bearings decreases slightly as the friction factor increases. This slight decrease can be attributed to the fact that the rotor and the inner race reach the same rotational speed earlier in the delevitation event. With the rotor and the inner race at the same speed the behavior of the rotor is essentially a rolling motion with minimal impacts.

The *Vvala* values seems to contradict the *Vval* values with a slight increase as the friction factor increases, when in fact this supports the previous claims. The initial behavior of the rotor will be more violent with increased friction between the contacting surfaces. With *Vvala* only having a window size of 1000 samples and only the maximum value for *Vvala* plotted in the graph, the plotted values show that the initial behavior of the rotor is more violent with increased friction. The more violent behavior is due to the rotor being forced to climb the walls of the bearing clearance producing a bouncing motion while the inner race speeds up to the rotor speed. The danger in using materials with a high friction factor is that the rotor can be forced into a backward whirling motion, with destructive consequences.

A possible conclusion that can be made from these results is that the friction between the rotor and the inner race should not be excessively high or low. A too low friction factor would cause the rotor to be more prone to forward whirling, while an excessively large friction factor could induce backward whirling.

In Figure 14 (B) the rotor sensitivity to the inertia of the inner race and balls of the rolling element bearing is shown. The sensitivity is similar to that of the friction, with the exception that the smaller window size *Vval* values seems insensitive to the variation in inertia of the rolling element bearing. This is due to the fact that even though the bearing takes longer to reach the same rotational speed as the rotor, the friction factor remains constant preventing an initial bouncing motion of the rotor.

When investigating the results from the longer window size *Vval* values it would appear that an ideal value for the inertia of the rolling element bearing would be 0, but this is not feasible. Another conclusion that can be made from this result is that it would be ideal if the rotor and the bearing inner race should have the same rotational speed at the moment of delevitation, but this is also not feasible. The inertia of the rolling element bearing is in effect causing a braking action on the rotor and with larger inertia the bearing takes longer to reach the same rotational speed as the rotor. Thus the braking action is present for a longer time period. This prolonged braking action causes the rotor to speed down quicker and the effect is that the rotor behavior over all is less destructive. Thus a bearing with a higher inertia would be preferential, due to the braking action applied to the rotor. The risk of using a bearing with an excessively large inertia is that the rotor could develop backward whirl should the friction force be sufficient and this risk is higher when the rotor traverses a critical speed.

These results are important when considering a rotor that is not actively braked in the event of a magnetic bearing failure. Should the rotor be actively braked the advantages of using a bearing with higher inertia is negated by the risk of causing backward whirling. In these cases it would be preferential to use a bearing with a small inertia to ensure that the bearing and rotor reach the same speed faster negating the possibility of developing backward whirl.

In Figure 14 (C) the sensitivity of the rotor behavior to the unbalance of the rotor is shown. From the results plotted in the graph it is clear that the rotor behavior is sensitive to the magnitude of the unbalance of the rotor.

While the plot shows that a lower unbalance would be preferential, this might not always be the case. Unbalance of a rotor has been showed to prohibit backward whirling of the rotor [4-6], while higher unbalance magnitudes tend to cause forward whirling [5-10]. Thus having a low unbalance present, in combination with a high friction factor and a bearing with a large inertia, might lead to the development of backward whirl. In general however a better balanced rotor is preferential, given that the backup bearings are rolling element type bearings, with neither an excessively large friction factor present between the contacting surfaces nor bearings with an excessively large inertia.

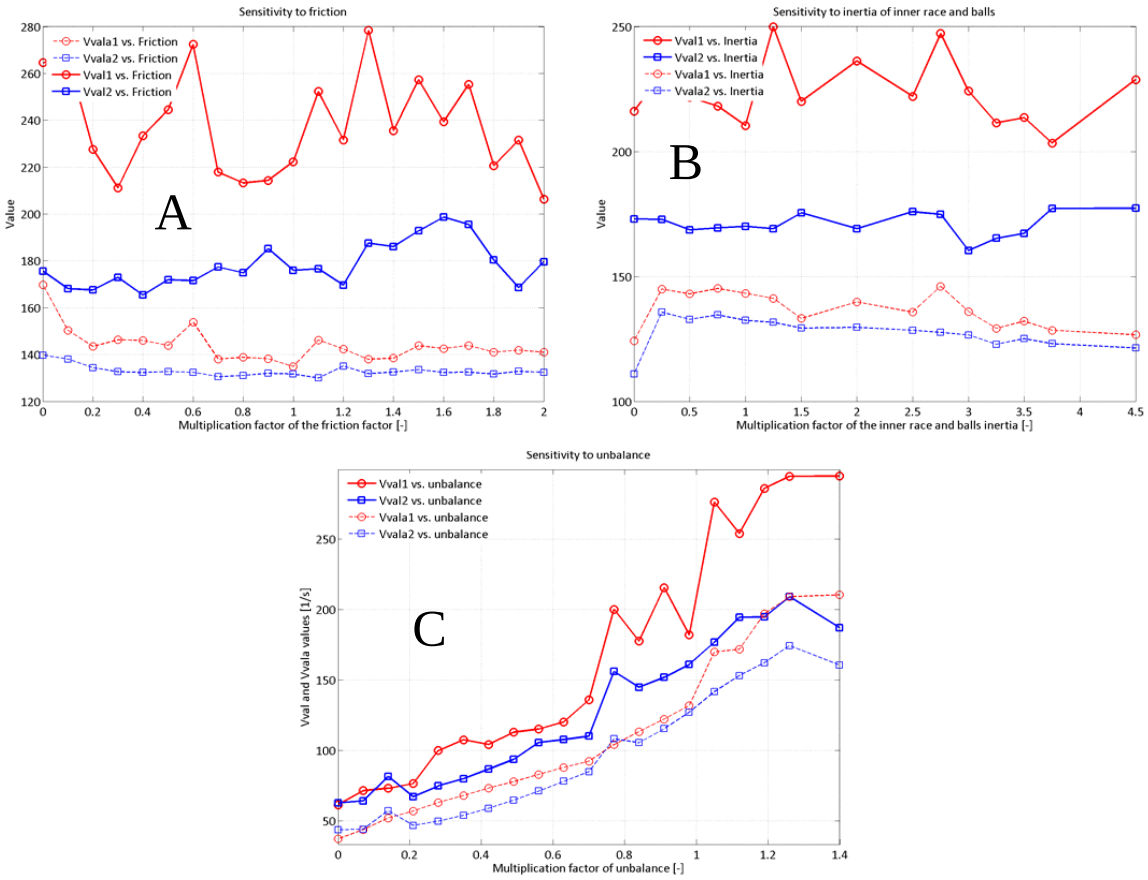

Figure 14: Rotor behavior sensitivity to:
(A) friction between the inner race of the rolling element bearings and the rotor contact surface
(B) inertia of the inner race and balls of the rolling element bearing
(C) unbalance of the rotor

5 Conclusion

A method to quantify the severity of a rotor drop event was presented (Vval), and verified using simulation and experimental results. *Vval* and *Vvala* values were used to verify the validity of the previously presented [1] simulation model BBSim. Experimental results were compared with simulated results, and similar behavior was observed in the simulated and experimental results.

The simulation (BBSim) was used to create parametric studies; the parametric studies revealed that the rotor behavior is determined by various parameters. The results of the parametric studies were analyzed and the following conclusions were made:

- Rotor behavior is less sensitive to bearing stiffness compared to bearing damping. Where a higher damping is preferential, with neither excessively large nor small bearing stiffness.

- Rotor behavior is found to be slightly sensitive to the delevitation angle, where the rotor behavior is adversely affected when the rotor is delevitated near the right side of the backup bearing clearance for a rotor rotating anti-clockwise, and near the left side for a rotor rotating clockwise.
- Rotor behavior is moderately sensitive to the friction factor between the contacting surfaces, where the friction factor should neither be too high nor too low, the friction factor of steel on steel of 0.2– 0.25 should be sufficient. Thus the need for extra surface lubrication is unnecessary.
- A higher inertia for the bearing is preferential for free running (not actively braked) rotors, where the speed-up of the bearing acts as a brake on the rotor. The contrary is preferential for actively braked rotors, where a lower inertia is preferred due to the possibility of developing backward whirl.
- Unbalance plays an important role in the behavior of the rotor, where a well-balanced rotor is preferred, given that the bearing inertia and the contact friction are not excessively large.

6 Shortcomings and future work

The shortcoming of the results shown is that the damping and stiffness values for the bearings and bearing enclosures were unknown, leading to results that do not exactly match the simulated results. Future work would include measuring the bearing and bearing housing stiffness and damping characteristics.

Another shortcoming of the presented work is that it is only done on one experimental system. Future work would include more experimental results on the same system as well as on other systems.

Using the results from various experimental systems *Vval* and *Vvala* values can be classified into rotor delevitation event severity classes.

References

[1] Jan J. Janse van Rensburg, George van Schoor, and Pieter A. van Vuuren, "Delevitation modelling of an active magnetic bearing supported rotor," in *Proceedings of the 12th International Symposium on Magnetic Bearings (ISMB12)*, Wuhan, China, 2010.

[2] C. Vanek, F. Worlitz, J. J. Janse van Rensburg, and G. van Schoor, "Experimentelle und theoretische Untersuchungen zum Rotorabsturz in Wälzlager," in *8. Workshop Magnetlagertechnik Zittau-Chemnitz*, Zittau, 2011, pp. 97-101.

[3] Eugén Otto Ranft, "The development of a flexible rotor active magnetic bearing system," North-West University Potchefstroom campus, Potchefstroom, Masters thesis 2005.

[4] G. Sun, A. B. Palazzolo, Andrew Provenza, and Gerald Montague, "Detailed Ball Bearing Model for Magnetic Suspension Auxiliary Service," *Journal of Sound & Vibration*, vol. 269, pp. 933-963, 2004.

[5] J. Schmied and J. C. Pradetto, "Behaviour of a One Ton Rotor Being Dropped Into Auxiliary Bearings," , 1992.

[6] Matthew T. Caprio, Brian T. Murphy, and John D. Herbst, "Spin Commissioning and Drop Tests of a 130 kW-Hr Composite Flywheel," , 2004.

[7] R. G. Kirk and T. Ishii, "Transient Rotor Drop Analysis of Rotors Following Magnetic Bearing Power Outage," , 1993.

[8] E E Swanson, R G Kirk, and J Wang, "AMB rotor drop initial transient on ball and solid bearings," in *Proc. MAG 95*, Alexandria, VA, USA, 1995, pp. 207-216.

[9] S Zeng, J Q Zhang, and H N Wang, "Transient response of active magnetic bearing rotor during rotor drop on backup bearings," *Proceedings of the Institution of Mechanical Engineers, Part C: Journal of Mechanical Engineering Science*, pp. 785-794, February 2006.

[10] Lawrence Hawkins, Alexei Filatov, Shamim Imani, and Darren Prosser, "Test Results and Analytical Predictions for Rotor Drop Testing of an Active Magnetic Bearing Expander/Generator," *Transactions of the ASME*, vol. 129, pp. 522-529, 2006.